

Determination of Cross Section for Different Fusion Reactions in Terms of Lattice Effects in Solid State Internal Conversion for Different metallic Crystalline Environments

S.N.Hosseini-motlagh¹, M.Shahamiri²

¹ Department of Physics, Shiraz branch Islamic Azad University, Shiraz, Iran

² Sama technical and vocational college, Islamic Azad University, Kazeroon Branch, Kazeroon , Iran

Abstract

In present paper, the cross section for $D(d,p)T$, $D(d,\gamma)^4\text{He}$, $T(d,n)^4\text{He}$ and $D(p,\gamma)^3\text{He}$ fusion reactions in terms of the lattice effect in solid state internal conversion for different structures and different metallic crystalline environments in comparison with palladium environment has been determined. Elements that we used in this article are Ni, Ru, Rh, Pt, Ta, Ti, Zr, which are contained FCC, BCC and HCP lattice structures. Fusionable particles are solved as a sublattice in mentioned crystalline metals. Fusion reactions are generated by flux of incoming fusionable particles. We took lattice effect part into our calculations with regarding the Bloch function for the initial and final state of three body system. Three-body system involved the host lattice, sublattice and incident particles. The cross section to perform each fusion reaction inside different metal is computed using the state of initial and final system. Then our results for cross section of different metal are compared with palladium metal. Finally, the solid state internal conversion coefficient is obtained by considering the lattice effect.

Key words: internal conversion, fusion cross section, lattice effect in solid state internal conversion

1. Introduction

Nowadays using nuclear energy is very important as a clean source of energy. There are two kinds of nuclear reactions, fusion and fission. Since fusion reaction has less radioactive radiation and the fusion fuels required for these reactions are more sufficiently available in the nature, therefore fusion reactions are important to study.

In 1995, many experimental works is done on gaseous metals for determining screening effect [1]. From 1998 to 2001, these experiments continued on metallic environments [2-4]. In 2000, the electron screening effect on cold fusion reaction was studied for $D + D$ in the metallic environment [5]. In 2002, they released a two-volume report, "Thermal and nuclear aspects of the Pd/D₂O system," with a plea for funding [6]. In 2002, the enhancement of cold fusion and solid state effect were studied in deuterated metal for $D+D$ [7]. From 2002 to 2004, the screening effect on 50 metals and insulator is checked by series of experiments [8-10]. In 2003, the enhancement of deuteron-fusion reactions in metals and experimental implications were studied for electron screening effect [11]. In 2004, the subject of solid state internal conversion came up [12]. In 2005, many efforts were done to make an apparatus according to the Fleischmann and Pons' works; finally, Cold fusion apparatus was made at San Diego Space and Naval Warfare Systems Center. They used other names instead of cold fusion to reduce the effect of previous

39 failures. Often they prefer to name their field **Low Energy Nuclear Reactions (LENR)** or
40 **Chemically Assisted Nuclear Reactions (CANR)**, also **Lattice Assisted Nuclear Reactions**
41 **(LANR)**, **Condensed Matter Nuclear Science (CMNS)** and **Lattice Enabled Nuclear**
42 **Reactions [13-16]**.

43 In 2002, Peter Kalman and Thomas Keszthelyi studied this problem (enhancing cross section)
44 on different metals. They studied many different factors to explain the enhancement of cross
45 section. For example, the electron screening was checked for 29 deuterated metals and 5
46 deuterated insulators/semiconductors from periodic tables. Among them, metals were most
47 convenient. Some of the other factors that they considered were: stopping power, thermal
48 motion, channeling, diffusion, conductivity, and crystal structure and electron configuration.
49 None of them could explain the observed enhanced cross section [7, 9, 11, 17-19]. In 2004, they
50 found a reason to explain the enhancement of cross section that was called solid state internal
51 conversion [12]. In 2008, screening effect is studied for the first time on metals by considering
52 solid state; actually solid state of metals is expressed in experiments [20]. Finally, in 2009, they
53 considered a metal with its lattice structure and entered the lattice shape of the solid in their
54 internal conversion calculations [21]. Their calculations were just for $D(p,\gamma)^3\text{He}$ reaction.

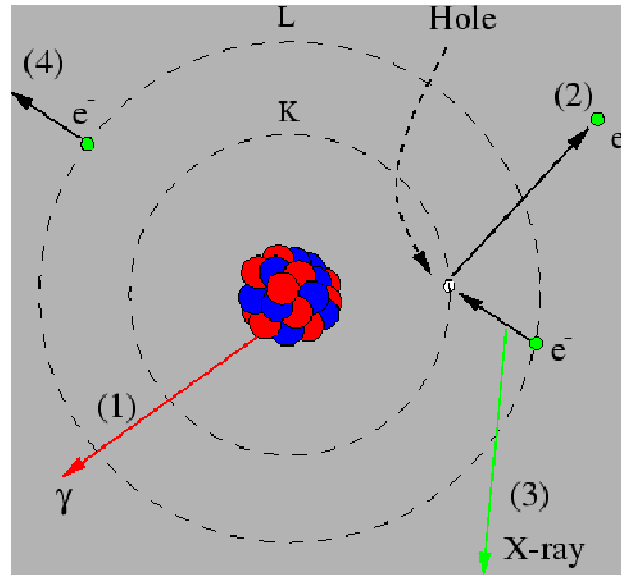
55 In this paper, different metals are considered. We choose such metals that are shown the best
56 results in term of screening effect and the density of deuterium [22]. In this article, in order to
57 compare internal conversion (IC) with lattice effect in solid state internal conversion (LEISSIC),
58 we calculate cross section for different seven ^3He particles plus palladium for $D(p,\gamma)^3\text{He}$, $D(d,p)\text{T}$,
59 $D(d,\gamma)^4\text{He}$, $\text{T}(d,n)^4\text{He}$.

60 The aim of this work is to determinate fusion cross section (FCS) for above reactions in different
61 metallic environments regarding LEISSIC in order to find the reason of enhanced FCS in these
62 metallic media then recommend the best metal. To approach this aim, following steps are
63 studied: First, right after introduction, the aspects of IC, SSIC and LEISSIC are explained.
64 Second, different special lattice such as Face Cubic Centered (FCC), Body Cubic Centered
65 (BCC) and Hexagonal close Packed (HCP) are introduced in details. Third, LEISSIC and other
66 required quantities to determinate FCS and LEISSIC coefficient for Pd environment are
67 computed. Fourth, all calculations in the third step are repeated for Ni, Ru, Rh, Pt, Ta, Ti, Zr.
68 Fifth, microscopic FCS for all elements are determined in different reaction for the case that
69 these metals are considered as host particle in lattice. Finally, we can suggest the best kind of
70 lattice, fusion reaction and metallic environment which have high value LEISSIC when cold
71 fusion happening.

72 2. Internal Conversion (IC) and Solid State Internal Conversion (SSIC)

73 Internal conversion is a radioactive decay process where an excited nucleus interacts with an
74 electron in one of the lower atomic orbitals, causing the electron to be emitted from the atom.
75 Thus, in an internal conversion process, a high-energy electron is emitted from the radioactive
76 atom, but without beta decay taking place. Since no beta decay takes place in internal
77 conversion, the element atomic number does not change, and thus (as is the case with gamma

78 decay) no transmutation of one element to another is seen. Also, no neutrino is emitted in
 79 internal conversion. Most internal conversion electrons come from the K shell (1s state, see
 80 electron shell), as these two electrons have the highest probability of being found inside the
 81 nucleus. After the electron has been emitted, the atom is left with a vacancy in one of the inner
 82 electron shells. This hole will be filled with an electron from one of the higher shells and
 83 subsequently a characteristic x-ray or Auger electron will be emitted [23,24]



84

85

Figure 1: Internal conversion

86 The enhancement in the fusion rate, which is observed in solid metallic environments, is
 87 attributed to the presence of solid state material but up till now the theoretical explanation of the
 88 phenomenon is still missing [25-27]. In what follows we suggest a possible mechanism called
 89 solid state internal conversion process that should be considered when trying to understand the
 90 extra fusion events. [28].

91

92 A similar process to IC can take place in a solid between fusible nuclei and any charged
 93 particle in the crystal. The solid state internal conversion process, e.g. $D(p,\gamma)^3\text{He}$ nuclear
 94 reaction, can be processes consisting of (a) a bound-free electron transition $p + d + (e) \rightarrow ^3\text{He} +$
 95 e and (b) a bound-free deuteron transition $p + d + (d) \rightarrow ^3\text{He} + d$. Therefore, as internal
 96 conversion happened in solid environment in addition of electron channel, we have deuteron
 97 channel too [12]. Increasing absorption is shown that in a solid material, nuclear fusion
 98 reactions (NFR) can happen in solid state internal conversion that creates transit for every
 99 charged particle by electromagnetic reaction [12].

100 3. Describing mentioned lattice structure in this article: FCC, BCC, HCP

101

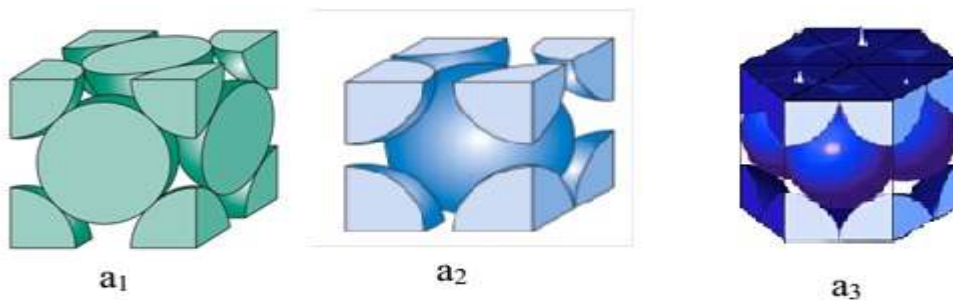
102 In this paper, these elements are studied: Ni, Ru, Rh, Pt, Ta, Ti, Zr. Which, Ni, Pt, Rh have a
 103 FCC lattice such as Pd. Ru, Ti, Zr have a HCP lattice and the lattice of Ta is BCC.

104 After investigating prior experimental work, finally in 2008 solids are considered without
105 their lattice crystal [20]. Then, in 2009, calculations are continued for Pd and with regarding the
106 crystalline lattice [21]. Before study on solid state internal conversion the scientists examined
107 screening effect on metals to finding the reasons of the enhancement FCS of metals which was
108 observed[22].In this article chosen element are significant in screening effect or deuterium
109 density. For example, Ti and Zr showed the most screening potential in the experiments [11]. Ta
110 and Zr had the most solved deuterium density [22]. Whereas having a maximum deuterium
111 density in Ti depends on having high temperature [12].

112 The most important quantities that change during calculations are unit cell volume and the
113 number of atom that belongs to each kind of lattice. Those quantities are explained for each
114 lattice that is following.

115 In each unit cell of FCC and BCC lattice, eight atoms stand on the corner of cubic that are
116 collaborative between eight other closed cubic (Fig 2, a_1 and a_2),thus, each unit cell has one atom
117 from corners ($8 \times \frac{1}{8} = 1$). For FCC there is one atom which belongs to two closed cubic but for
118 BCC one atom locates in the center of each unit cell. So, FCC and BCC lattice have respectively
119 3 atoms from all 6 sites ($6 \times \frac{1}{2} = 3$) and one atom from its center. Therefore, FCC and BCC
120 have four($1 + 3 = 4$) and two ($1 + 1 = 2$) atoms for each unit cell respectively.

121 HCP lattice: In each unit cell of HCP (see fig.2, a_3), there are two atoms on the top and down
122 sides that are shared between two closed unit cells ($2 \times \frac{1}{2} = 1$), on the other sides of the unit cell
123 there are six atoms. Each atom belong two closed unit cells($6 \times \frac{1}{2} = 3$). There are twelve atoms
124 in the corners that are collaborating between three closed unit cells($12 \times \frac{1}{3} = 4$). Consequently,
125 there are eight atoms that are completely belonging to one unit cell. In this lattice there are two
126 lattice constants: c height of unit cell and a, the face of hexagonal.



127

128

Figure 2: Shape of unit cell; a_1 : FCC unit cell, a_2 : BCC unit cell, a_3 : HCP unit cell.

129

The volume of unit cell for each lattice is defined by equation 1,

$$v_{cell} = \left\{ \begin{array}{ll} \frac{a^3}{4} & FCC \\ \frac{a^3}{2} & BCC \\ \frac{3\sqrt{3}}{16} a^2 c & HCP \end{array} \right\}, (a, c: \text{lattice constant}) \quad (1)$$

130

131

132 4. Lattice Effect in Solid State Internal Conversion

133 4.1. Cross section theory of LEISSIC

134 Since particles in the crystal are placed in specific sites, we can estimate fusion cross section
 135 (FCS) reactions using Block theorem for describing initial and final states of this system
 136 (palladium environment). In all formulas subscripts 1, 2 and 3 are respectively pointed at
 137 incoming, sublattice and host particles. Also, the state of particles in the lattice is determined by
 138 Block function [28]

$$139 \varphi_{k_3,i}(r_3) = \frac{1}{\sqrt{N}} \sum_{l_s} e^{ik_3 \cdot l_s} a_3(r_3 - l_s - u_3(l_s)) \quad (2)$$

140 where, r_3 , $k_{3,1}$ and a_3 are respectively introduced host-particle coordinate, a wave vector of the first
 141 Brillouin zone of the reciprocal lattice, and Wannier function. Here, Pd (palladium), d (duetron)
 142 and e (electron) are considered as host particles. Lattice site and the displacement of the atom
 143 located at lattice site are symbols to represent l_s and $u_3(l_s)$. Here N is the number of lattice
 144 point. The sublattice particle also is described by Block function (Eq3). Lattice contains N_2
 145 fusionable particles, for palladium system it is assumed that $N_2 = N$.

$$146 \varphi_{k_2,i}(r_2) = \frac{1}{\sqrt{N_2}} \sum_{l_s} e^{ik_2 \cdot l_s} a_2(r_2 - l_s - u_2(l_s)) \quad (3)$$

147 Here, a_2 and a_3 are Wannier functions for sublattice and host particles respectively that are determined
 148 by equation 4[20],

$$a_j(x) = \left(\frac{\beta_j^2}{\pi} \right)^{3/4} e^{-\frac{\beta_j^2}{2} x^2} (x = r_2 - l_s), j = 2,3 \quad (4)$$

149 In the above formula, $\beta_j = \sqrt{m_j \omega_j / \hbar}$ [6]. The initial state Ψ_i for the three particles that participate
 150 in solid state assisted fusion reaction is described by,

$$151 \Psi_i = \varphi_{k_2,i}(r_2) \varphi_{k_3,i}(r_3) \varphi_1(r_1 - r_2) \quad (5)$$

152 where, $\varphi_1(r_1 - r_2)$ is the Coulomb wave function corresponding to the state of a sublattice and
 153 incoming particle. The Coulomb wave function is [20],

$$\varphi_1(r_1 - r_2) = e^{ik_1 \cdot (r_1 - r_2)} \frac{f(k_1, r_1 - r_2)}{\sqrt{V}} \quad (6)$$

154 V is the volume of normalization, k_1 is the wave vector, r_1 is the coordinate of incoming particle,
 155 and f function is defined as the following:

$$156 f(k_1, x) = e^{-\pi\eta/2} \Gamma(1 + i\eta) {}_1F_1(-i\eta, 1; i[k_1 x - \mathbf{k}_1 \cdot \mathbf{x}]) \quad (7)$$

157 ${}_1F_1$ is the confluent hyper geometric function [4]. η is determined by using the eq. 8 and 9 [29].

$$\eta = 0.1575 z_1 z_2 \left(\frac{A}{E}\right)^{1/2} \quad (8)$$

$$A = \frac{A_1 A_2}{A_1 + A_2} (amu) \quad (9)$$

158 where z_1 and z_2 are the charge number of particles 1 and 2 and E is the energy of incoming
 159 particle. A_1 and A_2 are the mass of incident and sublattice particles that are measured in amu unit.
 160 The final state of this three- body system is defined by,

$$161 \Psi_f = \psi_f(r_1, r_2) \varphi_f(r_3) F_{Cb}(z_3, z_{12}, v_{3,12}) \quad (10)$$

162 Where φ_f is a plane wave of wave vector k_3 that is corresponded to an outgoing particle 3.

$$162 \varphi_f(r_3) = \frac{1}{\sqrt{V}} e^{ik_3 \cdot r_3} \quad (11)$$

163 ψ_f stands for the outgoing fusion product leaving a deuteron lattice point vacant that is given in
 164 the relative coordinate ($r = r_1 - r_2$) and the center of mass coordinate ($R = m_1 r_1 + m_2 r_2 / m$) of the
 165 particles of the rest masses m_1 and m_2 then we have,

$$166 \psi_f(r, R) = \frac{1}{\sqrt{V}} e^{iK \cdot R} \chi(r) \quad (12)$$

167 where K and $\chi(r)$ are the wave vector of fusion product and a nuclear wave function,
 168 respectively.

$$\chi(r) = \left(\frac{\lambda^2}{\pi}\right)^{3/4} e^{-\lambda^2 r^2 / 2} \quad (13)$$

169 We determine the Coulomb interaction between host particle and the product of the incident and
 170 sublattice reaction using the Fermi correction;

$$171 F_{Cb} = \sqrt{2\pi\xi} \frac{e^{-\pi\xi}}{\sqrt{1-e^{-2\pi\xi}}} \quad (14)$$

172 Where, $\xi = z_3 z_{12} \alpha_f \sqrt{\mu c^2 / 2Q}$ and α_f is the fine structure constant. μ is the reduced mass

$$\mu = \frac{(m_1 + m_2) m_3}{m_1 + m_2 + m_3} \quad (15)$$

173 The element of s-matrix that is used for determining of the cross section of the different fusion
 174 reaction is known as,

$$175 S_{fi} = \frac{2\pi}{i\hbar} \iiint \Psi_f^* \frac{z_1 z_3 e^2}{|r_1 - r_3|} \Psi_i d^3 r_1 d^3 r_2 d^3 r_3 \delta(E/\hbar) \quad (16)$$

176 With a little simplification on this integral and using the HatreeFok approximation for Coulomb
 177 interaction part of integral, we have

$$178 \frac{z_1 z_3 e^2}{|r_1 - r_3|} = \frac{z_1 z_3 e^2}{2\pi^2} \int d^3 q \frac{1}{q^2} e^{iq \cdot (r_1 - r_2)} \quad (17)$$

179 Putting the Fourier transform of Eq.12 in Eq.15 , and applying the approximation 16 and
 180 comparing it with $\langle\sigma v\rangle$ formula , the cross section of fusion reaction between host and target
 181 fusional particles is obtained as the following ,

$$\sigma_2 = C_0 \frac{\exp(-2\pi\eta)}{E} \quad (18)$$

182 E is the energy of incoming particle and C_0 is determined by,

$$C_0 = |F_{cb}|^2 A_0 k_\mu \left(\frac{\beta_2}{K_Q}\right)^3 \langle|\tilde{\chi}|_{K=K_Q}^2\rangle_{\Omega_K} \quad (19)$$

184 With Ω_K denoting the solid angle in the K space, $\beta_2 = \sqrt{m_d \omega / \hbar}$, $A_0 = 128 \alpha_f^3 z_1^3 z_3^2 z_2 m_1 c^2 \sqrt{\pi}$,
 185 $K_Q = \sqrt{2\mu c^2 Q} / (\hbar c)$, Q is the energy of the reaction, $k_\mu = \mu c / \hbar$. The average of nuclear wave
 186 function is defined by,

$$\langle|\tilde{\chi}|_{K=K_Q}^2\rangle_{\Omega_K} = \left|\tilde{\chi}\left(\frac{m_2}{m}K\right)\right|^2 = \frac{8\pi^{3/2}}{\lambda^3} e^{-\frac{4K^2}{9\lambda^2}} \quad (20)$$

187 m_n , nucleons mass, ω_n angular frequent of binding energy are calculated for each reaction
 188 separately (table 4).

$$\lambda = \frac{\sqrt{m_n \omega_n}}{\hbar} \quad (21)$$

$$m_n = m_i + m_{He}, i = d \text{ or } t \quad (22)$$

$$\omega_n = \frac{\text{binding energy of He(MeV)}}{\hbar} \quad (23)$$

189 Here, C_0 is calculated for one d or one Pd. In order to compare C_0 with astrophysical factor (S(0)) in
 190 ordinary state , it must be calculated considering the density of these particles. So, we use the
 191 Eq.23,

$$NC_0 = A\Delta R_h C_1 \quad (24)$$

192 In this case, N is defined by,

$$N(Pd) = V_{eff} / v_{cell} \quad (25)$$

193 Where $v_{cell} = d^3 / 4$, $V_{eff} = A\Delta R_h$ and $d = 3.89 \times 10^{-8} \text{cm}$ is the lattice constant

$$N(d) = u V_{eff} / v_{cell} \quad (26)$$

194 In Eq.26, u is the ratio of deuteron to palladium number density. For electron $u = 10$ which is the
 195 number of electron valence in palladium. C_0 contains all the properties of the lattice. For
 196 comparison the fusion cross section with and without LEISSIC we have to determine the
 197 macroscopic cross section.

$$\Sigma = N\sigma_2 \quad (27)$$

199 4.2. Results of numerical calculations for each reaction

200 There are two tables for all reactions that can aid in plotting the cross section and comparing
 201 with the ordinary state. The suppositions of host, sublattice and incoming particles are expressed
 202 for all reactions in this way: the host particles are Pd,d,e for Palladium. The sublattice is
 203 deuterium for all reactions. The incoming particles are proton (p) in $D(p,\gamma)^3\text{He}$, deuterium (d) in
 204 $D(d,p)\text{T}$ and $D(d,\gamma)^4\text{He}$ and tritium (t) in $T(d,n)^4\text{He}$. Our calculation for obtaining the cross

205 section for all three kind of host particles are accomplished by using equations: 12,13,17,19 and
 206 our obtained results are given in tables 1 and 2.

207 *Table 1: our numerical calculation of necessary quantities for obtaining C_0 for all chosen reactions*

Type of Reactions	host particles	$A_0(\text{MeV})$	$\mu(\text{gr})$	$K_Q(\text{cm}^{-1})$	$ \tilde{\chi} _{K=K_Q}^2 (\text{cm}^3)$	ξ
D(p,γ)3He	Pd	175	5.013×10^{-24}	8.91×10^{12}	3.95×10^{-38}	10.755
	d	0.0827	2.005×10^{-24}	5.64×10^{12}	5.13×10^{-38}	0.1477
	e	0.0103	-----	2.78×10^{11}	6.11×10^{-38}	-560382
D(d,p)T	Pd	349	6.686×10^{-24}	8.82×10^{12}	3.15×10^{-38}	14.462
	d	0.165	2.229×10^{-24}	5.09×10^{12}	3.97×10^{-38}	0.181
	e	0.021	-----	2.05×10^{11}	4.45×10^{-38}	-0.0011
D(d,γ)4He	Pd	349	6.686×10^{-24}	7.93×10^{12}	3.69×10^{-38}	16.075
	d	0.165	2.229×10^{-24}	4.58×10^{12}	4.51×10^{-38}	0.202
	e	0.021	-----	1.65×10^{11}	4.98×10^{-38}	-0.0022
T(d,n)4He	Pd	524	8.35×10^{-24}	2.05×10^{13}	2.89×10^{-39}	5.863
	d	0.248	2.387×10^{-24}	1.10×10^{13}	4.24×10^{-39}	0.09
	e	0.031	-----	8.90×10^{11}	4.30×10^{-38}	-4.228

208

209 From the results of table 1 and Eqs. 17 and 27 for different reactions and host particle, we can
 210 calculate the required parameters such as C_0 and C_1 which are important for estimating cross
 211 section of the fusion reactions.

212 *Table 2: our numerical calculation C_0 and C_1 for different host particle and different reactions*

Type of Reactions	host particles	$k_\mu (\text{cm}^{-1})$	$ F_{cb} ^2$	$C_0 (\text{MeV b})$	$C_1 (\text{MeV b})$
D(p,γ)3He	Pd	1.42×10^{14}	3.14×10^{-28}	4.92×10^{-38}	3.36×10^{-24}
	d	0.57×10^{14}	0.61	2.30×10^{-13}	$u \times 15.6$
	e	-----	1	9.10×10^{-13}	6.18×10^2
D(d,p)T	Pd	1.90×10^{14}	3.27×10^{-38}	1.11×10^{-47}	7.53×10^{-34}
	d	0.63×10^{14}	0.5371	1.88×10^{-13}	$u \times 12.78$
	e	-----	1	2.48×10^{-12}	1.687×10^3
D(d,γ)4He	Pd	1.90×10^{14}	7.02×10^{-41}	3.83×10^{-50}	0.26×10^{-35}
	d	0.63×10^{14}	0.4964	2.70×10^{-13}	$u \times 18.35$
	e	-----	1	4.31×10^{-36}	2.93×10^{-21}
T(d,n)4He	Pd	2.37×10^{14}	4.44×10^{-15}	2.05×10^{-25}	1.39×10^{-12}
	d	0.68×10^{14}	0.7438	4.45×10^{-15}	$u \times 0.3024$
	e	-----	1	1.87×10^{-13}	127.1

213

214 Since each palladium unit cell has 4 Pd atoms purely and since we suppose that the number of
 215 host and sublattice particles are equal, then we have

$$N_{Pd} = \frac{1}{4} \times 4.22 \times 10^{22} \quad (28)$$

216 The other quantities such as $\alpha_{m,n}$, β_2 and Q which is mentioned before are calculated and
 217 numerical results are summarized in table 3.

218 *Table 3: our obtaining required quantities which are calculated for determination of different fusion*

Type of Reactions	λ (cm ⁻¹)	β_2 (cm ⁻¹)	Q (MeV)	Binding Energy (MeV)
D(p, γ) ³ He	9×10^{12}	4.81×10^{14}	5.49	7.718
D(d,p)T	10×10^{12}	4.81×10^{14}	4.04	8.482
D(d, γ) ⁴ He	9.63×10^{12}	4.81×10^{14}	3.27	28.3
T(d,n) ⁴ He	21.8×10^{12}	4.81×10^{14}	17.59	28.3

219

220 4.3. Calculations the solid state internal conversion coefficient for different 221 fusion reactions in Palladium crystal environment

222 With regarding to definition that exists in Ref.11, we can write $v_{eff} = A\Delta R_h$, where A is the
 223 cross section of the beam, ΔR_h is the “differential” range, that is, the distance within which the
 224 energy of the incoming particle can be considered unchanged. The $\Delta R_h \ll R_h$ condition helps in
 225 an order of magnitude estimate of ΔR_h , where R_h is the stopping range of a proton which is
 226 about $8 \times 10^{-2} \mu m$ at $E = 0.01 MeV$ in Pd [22]. The quantities A and R_h were measured in
 227 mm^2 and $10^{-3} \mu m$ units. The solid state internal conversion coefficient is introduced as,

$$\alpha_{SSIC} = A\Delta R_h C_1 / S(0) \quad (29)$$

228 $S(0)$ is the astrophysical factor and the amounts of $S(0)$ were calculated completely in the ref [27].
 229 Here since the issue is studied on the low energy (5-30 eV), the amounts of $S(0)$ for each
 230 reaction is a constant that are shown in table 4.

231 *Table 4: the amounts of astrophysical S-factor for different reactions in ordinary state in low energy*

232

Reactions	D(p, γ) ³ He	D(d,p)T	D(d, γ) ⁴ He	T(d,n) ⁴ He
Astrophysical factor				
S(0) MeV barn	0.2×10^{-6}	0.056	0.054	10

236

237 By using the amounts exist in tables 2, 4 and replacing them into Eq.28 the solid state internal
 238 conversion coefficient for different reactions can be found. This coefficient indicates the internal
 239 conversion rate in different reactions. The result of the calculations summarize in table 5.

240 *Table 5: solid state internal conversion coefficient in different reactions for e, 4d and d channels*

Type of reactions	$\alpha_{SSIC,d} A\Delta R_h$	$\alpha_{SSIC,e,4d} A\Delta R_h$
-------------------	-------------------------------	----------------------------------

$D(p,\gamma)^3\text{He}$	$u \times 7.8 \times 10^5$	3.1×10^9
$D(d,p)\text{T}$	$u \times 3.03 \times 10^4$	3.2×10^6
$D(d,\gamma)^4\text{He}$	$u \times 3.398 \times 10^2$	5.42×10^{-20}
$T(d,n)^4\text{He}$	$u \times 0.03$	12.7

241

242 We find out the solid state internal conversion happens in $D(p,\gamma)^3\text{He}$ and $D(d,p)\text{T}$ reactions with
 243 more rates. All calculations in this part are shown for palladium. In the next part we show the
 244 results for other elements in detailed.

245 5. Calculations of LEISSIC for other elements

246 5.1. Tables of Calculation for Different Elements and Reactions

247 By using all formulas in section 3, such as what we have done for palladium, all required
 248 quantities can be computed for mentioned elements. Because other host particles (deuterium and
 249 electron) don't change in these calculations and the only thing that changes is the first row of the
 250 Table.1. Meanwhile, C_1 and C_0 which changes only for the elements are respectively showed in
 251 Table 6 and 7.

252 Table 6: Our numerical calculations of C_0 for different elements and reactions with FCC, BCC and HCP lattice

Quantity elements	$C_{0,D(p,\gamma)^3\text{He}}$ (MeV barn)	$C_{0,D(d,p)\text{T}}$ (MeV barn)	$C_{0,D(d,\gamma)^4\text{He}}$ (MeV barn)	$C_{0,T(d,n)^4\text{He}}$ (MeV barn)
Pd (FCC)	4.92×10^{-38}	1.11×10^{-47}	3.83×10^{-50}	2.05×10^{-25}
Ni (FCC)	3.44×10^{-27}	6.79×10^{-33}	2.56×10^{-35}	6.98×10^{-23}
Pt (FCC)	1.34×10^{-57}	1.95×10^{-74}	1.21×10^{-81}	1.63×10^{-45}
Rh (FCC)	1.08×10^{-36}	7.43×10^{-47}	6.61×10^{-51}	1.38×10^{-24}
Ru (HCP)	8.49×10^{-37}	5.07×10^{-46}	5.56×10^{-50}	1.21×10^{-30}
Ti (HCP)	1.10×10^{-23}	4.63×10^{-28}	6.49×10^{-30}	1.93×10^{-21}
Zr (HCP)	2.25×10^{-34}	1.01×10^{-42}	2.69×10^{-46}	6.27×10^{-29}
Ta (BCC)	1.30×10^{-54}	3.10×10^{-70}	5.79×10^{-77}	2.64×10^{-43}

253

254

255

256

257 Table 7: Our numerical calculations of C_1 for different elements and reactions with FCC, BCC and HCP lattice

quantity				
----------	--	--	--	--

elements				
Pd (FCC)	Pd	3	7	
	d			
	e			
Ni (FCC)	Ni	3	6	
	d			
	e			
Pt (FCC)	Pt	6	7	
	d			
	e			
Rh (FCC)	Rh	7	4	
	d			
	e			
Ru (HCP)	Ru	5	2	
	d			
	e			
Ti (HCP)	Ti	5	2	
	d			
	e			
Zr (HCP)	Zr	8	2	
	d			
	e			
Ta (BCC)	Ta	7	2	
	d			
	e			

258

259 For comparing C_0 , the **microscopic**FCS of these metallic environments for all elements,
 260 numerical values from Table.6 can be useful. For studying the comparison of the C_1 quantity see
 261 table 7.

262 According to table 7, we find out that: wherever elements themselves are considered as host
 263 particles, the results of C_1 from large too small values for all reactions are: Ti, Ni, Zr, Ru, Rh, Pd,
 264 Ta and Pt. For cases that deuterium and electron are host particles, our comparing values lead to
 265 Ru, Ni, Ti, Rh, Pd, Pt, Zr, Ta and Ni, Ru, Pd, Pt, Rh, Ti, Ta,Zr respectively. In case that electron
 266 is host the number of electrons in capacity layer is too important indeed whatever the numbers of
 267 electrons increases the screening effect is enhanced. Between all reactions, $D(p,\gamma)^3\text{He}$, $D(d,p)\text{T}$
 268 and $D(d,\gamma)^4\text{He}$ have larger values of C_1 than $T(d,n)^4\text{He}$.

269 (According Table.7 the result of comparing C_1 for different host particles in different metallic
 270 environments are: element host particle, $C_{1,Ti} > C_{1,Ni} > C_{1,Zr} > C_{1,Ru} > C_{1,Rh} > C_{1,Pd} > C_{1,Ta} >$
 271 $C_{1,Pt}$; deuterium host particle, $C_{1,Ru} > C_{1,Ni} > C_{1,Ti} > C_{1,Rh} > C_{1,Pd} > C_{1,Pt} > C_{1,Zr} > C_{1,Ta};$
 272 electron host particle, $C_{1,Ni} > C_{1,Ru} > C_{1,Pd} > C_{1,Pt} > C_{1,Rh} > C_{1,Ti} > C_{1,Ta} > C_{1,Zr}$)

273

Table 8: Our numerical calculations of LEISSIC for all elements in different reactions

quantity elements				
Pd (FCC)	d	u	u	
	e			
Ni (FCC)	d	u	u	
	e			
Pt (FCC)	d	u	u	
	e			
Rh (FCC)	d	u	u	
	e			
Ru (HCP)	d	u	u	
	e			
Ti (HCP)	d	u	u	
	e			
Zr (HCP)	d	u	u	u
	e			
Ta (BCC)	d	u	u	
	e			

274

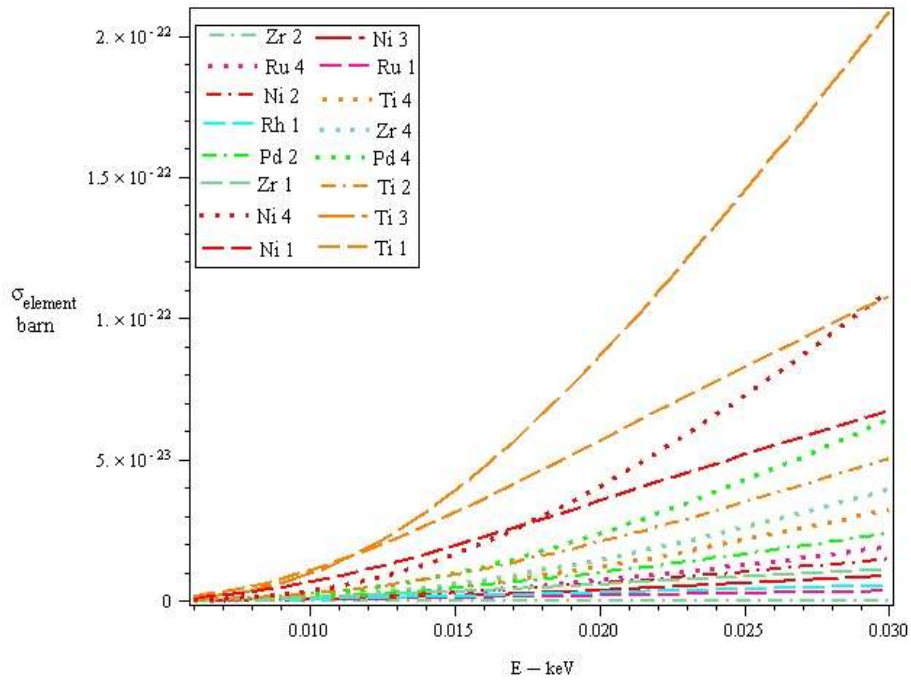
275 In the each environment, IC coefficient shows internal conversion rate and determined the cross
 276 section enhancement in each environment. By studying table 8, we find out that the internal
 277 conversion coefficient of deuterium for $D(p,\gamma)^3\text{He}$ is the largest one. IC coefficient for $D(p,\gamma)^3\text{He}$
 278 for different reactions from larger to smaller value is: Ru, Ni, Rh, Pt, Zr, Ta, Ti and Pd. As you
 279 see in this reaction Pd has the last rank. In $D(d,p)\text{T}$, the arrangement of the elements is: Pd, Ru,
 280 Ni, Ti, Rh, Pt, Zr and Ta.

281 Electronic internal conversion coefficient arrangement for different elements is: Ni, Ru, Pd, Rh, Ti,
 282 Ta, Zr, Pt. ($\alpha_{e,\text{Ni}} > \alpha_{e,\text{Ru}} > \alpha_{e,\text{Pd}} > \alpha_{e,\text{Rh}} > \alpha_{e,\text{Ti}} > \alpha_{e,\text{Ta}} > \alpha_{e,\text{Zr}} > \alpha_{e,\text{Pt}}$)

283 (According to Table.8, comparing ICC values of deuterium host particle for the two largest
 284 reactions $D(p,\gamma)^3\text{He}$ and $D(d,p)\text{T}$ are respectively: $\alpha_{d,\text{Ru}} > \alpha_{d,\text{Ni}} > \alpha_{d,\text{Rh}} > \alpha_{d,\text{Pt}} > \alpha_{d,\text{Zr}} > \alpha_{d,\text{Ta}} >$
 285 $\alpha_{d,\text{Ti}} > \alpha_{d,\text{Pd}}$ and $\alpha_{d,\text{Pd}} > \alpha_{d,\text{Ru}} > \alpha_{d,\text{Ni}} > \alpha_{d,\text{Ti}} > \alpha_{d,\text{Rh}} > \alpha_{d,\text{Pt}} > \alpha_{d,\text{Zr}} > \alpha_{d,\text{Ta}}$)

286 6. Microscopic cross section for all elements in different reactions

287 Microscopic FCS for all metallic environments when metal considers as a host particle are plotted
 288 by replacing numerical values in Table 6 and Eq.16. All FCS are divided into two groups in
 289 order to show changes clearly: 16 maximum and 16 minimum which are respectively shown in
 290 Fig 3 and Fig 4. Numbers 1 to 4 besides the name of the elements shows $D(p,\gamma)^3\text{He}$, $D(d,p)\text{T}$,
 291 $D(d,\gamma)^4\text{He}$ and $T(d,n)^4\text{He}$.



292

293

Figure3:16 maximum of microscopic FCS in terms of incoming energy for all reactions

294

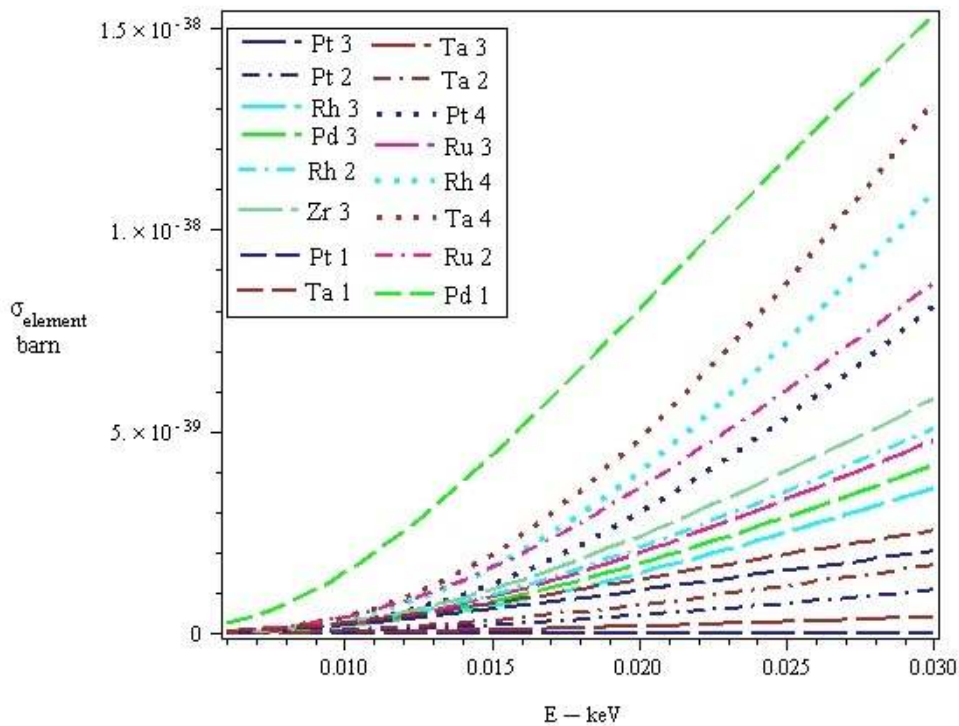
In the above graph, different colors shows kinds of elements and the styles of shape introduce kinds of reactions. $D(p,\gamma)^3\text{He}$ by “dash”, $D(d,p)\text{T}$ by “dashdot”, $D(d,\gamma)^4\text{He}$ by “longdash” and $T(d,n)^4\text{He}$ by “dot” are shown. The color of Pd, Ni, Pt, Rh, Ru, Ti, Zr, and Ta are respectively: Green, red, navy, cyan, dark pink, coral, aquamarine and brown. As you see Ti and Ni have the larger cross section. After them palladium shows up just in the $T(d,n)^4\text{He}$ reaction.

295

296

297

298



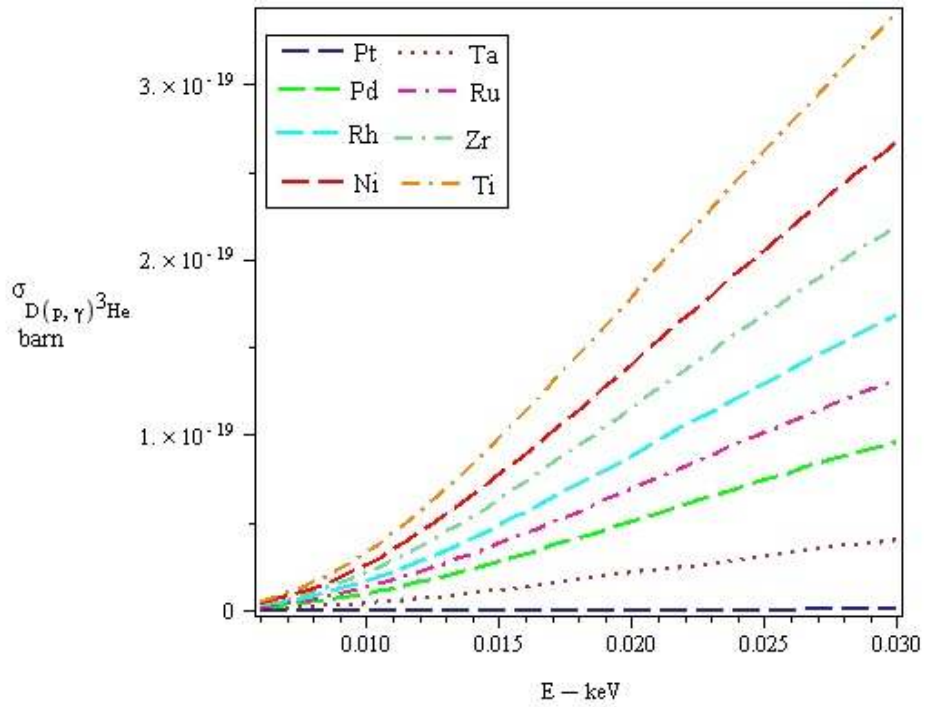
299

300

Figure 4: 16 minimum of micFCS in terms of incoming energy for all reactions

301 To realize the best kinds of lattice structure, **microscopic**FCS related to element host particles are
 302 plotted for each fusion reactions separately. **Here** in these graphs colors shows kinds of elements
 303 and the styles of the graph indicate the kind of the lattice. BCC **shows** by “dot”, FCC by “long
 304 dash” and HCP by “dashpot”.

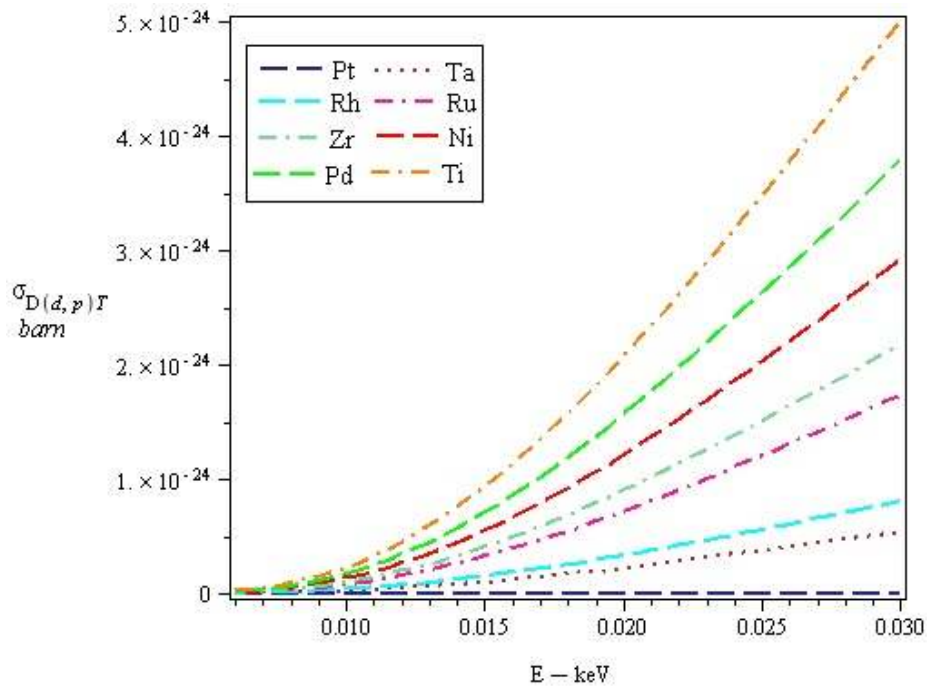
305



306

307

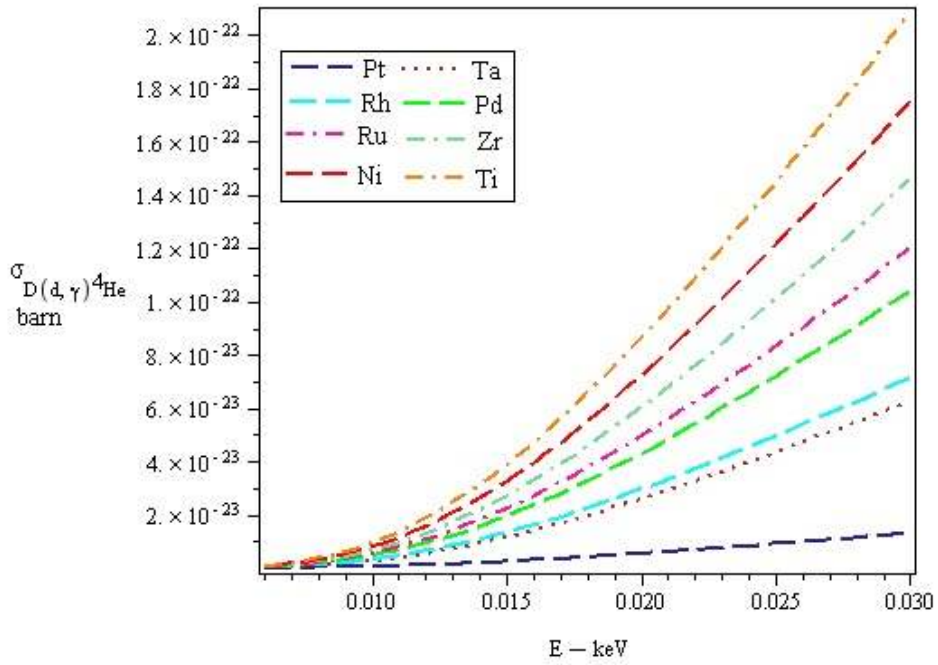
Figure 5: **Microscopic**FCS of all elements for $D(p,\gamma)^3\text{He}$.



308

309

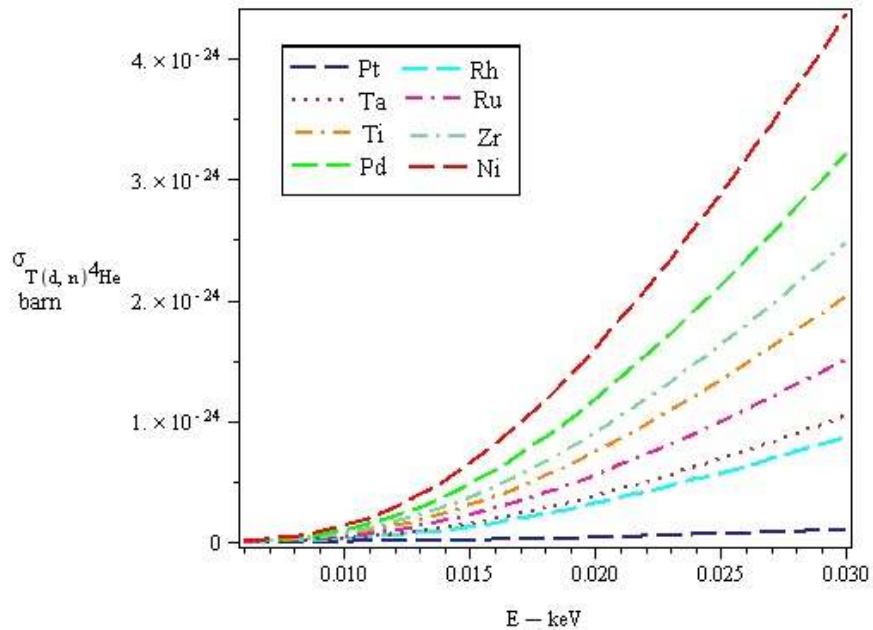
Figure 6: **Microscopic**FCS of all elements for $D(d,p)T$



310

311

Figure 7: Microscopic FCS of all elements for D(d,γ)4He



312

313

Figure 8: Microscopic FCS of all elements for T(d,n)4He

314

315

316

317

318

319

For D(p,γ)³He, D(d,p)T, D(d,γ)⁴He (Figs. 5,6,7 and 8), Ti with HCP lattice has the largest microscopic FCS and Pd with FCC lattice is respectively in the sixth, second and fifth place. From Fig.8 we can understand that Ni with FCC lattice is in the first place of microscopic FCS and Pd is the fifth. Now the data that are correspond to figures 3 and 4 are summarized in table 9.

320 Table 9: numerical microscopic cross sectioned values in special energy (0.025MeV) for different elements in
 321 different reactions

322

323

324

325

quantity elements	D(p, γ) ³ He (MeV)	D(d,p)T (MeV)	D(d, γ) ⁴ He	T(d,n) ⁴ He (MeV)
Pd (FCC)	1	8	2	8
Ni (FCC)	4	5	1	2
Pt (FCC)	2	1	9	6
Rh (FCC)	2	5	5	5
Ru (HCP)	3	3	4	5
Ti (HCP)	3	3	4	7
Zr (HCP)	4	7	2	2
Ta (BCC)	4	2	4	1

326

327

328

329

330

331

332

333

7. Discussion and Conclusion

334

335 According to table.7, the result of comparing C_1 for different host particles in different metallic
 336 environments are: when the metals are considered as host particle, $C_{1,Ti} > C_{1,Ni} > C_{1,Zr} >$
 337 $C_{1,Ru} > C_{1,Rh} > C_{1,Pd} > C_{1,Ta} > C_{1,Pt}$; whenever deuterium considered a host particle, $C_{1,Ru} >$
 338 $C_{1,Ni} > C_{1,Ti} > C_{1,Rh} > C_{1,Pd} > C_{1,Pt} > C_{1,Zr} > C_{1,Ta}$; electron host particle, $C_{1,Ni} > C_{1,Ru} >$
 339 $C_{1,Pd} > C_{1,Pt} > C_{1,Rh} > C_{1,Ti} > C_{1,Ta} > C_{1,Zr}$.

340 As you see in table.9 the best cross sections belong to D(p, γ)³He and D (d,p)T reactions. In order
 341 to achieve our goals we need to look back to our data about internal conversion coefficient by
 342 considering lattice effect.

343 In table 8, we find out that the internal conversion coefficient of deuterium for D (p, γ)³He is the
 344 largest one. IC coefficient for D(p, γ)³He for different reactions from larger to smaller value is:
 345 Ru, Ni, Rh, Pt, Zr, Ta, Ti and Pd. As you see in this reaction Pd has the last ICC. In D (d,p)T, the
 346 arrangement of the elements is: Pd, Ru, Ni, Ti, Rh, Pt, Zr and Ta.

347 Electronic internal conversion coefficient arrangement for different elements is: Ni, Ru, Pd, Rh,
 348 Ti, Ta, Zr, Pt. ($\alpha_{e,Ni} > \alpha_{e,Ru} > \alpha_{e,Pd} > \alpha_{e,Rh} > \alpha_{e,Ti} > \alpha_{e,Ta} > \alpha_{e,Zr} > \alpha_{e,Pt}$)

349 According to Table.8, comparing ICC values of deuterium host particle for the two largest
350 reactions $D(p,\gamma)^3\text{He}$ and $D(d,p)\text{T}$ are respectively: $\alpha_{d,Ru} > \alpha_{d,Ni} > \alpha_{d,Rh} > \alpha_{d,Pt} > \alpha_{d,Zr} > \alpha_{d,Ta} >$
351 $\alpha_{d,Ti} > \alpha_{d,Pd}$ and $\alpha_{d,Pd} > \alpha_{d,Ru} > \alpha_{d,Ni} > \alpha_{d,Ti} > \alpha_{d,Rh} > \alpha_{d,Pt} > \alpha_{d,Zr} > \alpha_{d,Ta}$)

352 As you see Ti and Ni have the larger cross section. After them palladium shows up just in the
353 $T(d,n)^4\text{He}$ reaction.

354 Looking at figs 5, 6, 7 and 8, can show that what the best lattice, kinds of environment and kinds
355 of reactions are. Ti with HCP lattice has the largest micFCS and Pd with FCC lattice is
356 respectively in the sixth, second and fifth place. From Fig.8 we can understand that Ni with FCC
357 lattice is in the first place of micFCS and Pd is the fifth. FCC and HCP are the best lattice
358 structures and Ti and Ni are best elements, Ru has a largest ICC In the case that deuterium is the
359 host particle.

By comparing FCS in term of LEISSIC, Ti and Ni show maximum data. By comparing integral
conversion coefficient in term of LEISSIC, the best results belong to Ni and Ru. So Ni can be the
best option for the next experimental works. We can neglect Ta and the BCC lattice because of
its worse results. 363

364 The other investigations show that: FCC and HCP lattice have a much closed results. Palladium
365 shows good results just in the $D(p,\gamma)^3\text{He}$ and $D(d,\gamma)^4\text{He}$.

References 366

- 367 [1] C. Rolfs and E. Somorjai, Nucl. Instrum. Methods B **99**, 297 (1995).
- 368 [2] K. Czerski, A. Huke, P. Heide, M. Hoefl, and G. Ruprecht in *Nuclei in the Cosmos V, Proceedings of*
369 *the International Symposium on Nuclear Astrophysics*, edited by N. Prantzos and S. Harissopulos
370 (Editions Frontieres, Volos, Greece, 1998) p. 152.
- 371 [3] K. Czerski, A. Huke, A. Biller, P. Heide, M. Hoefl, and G. Ruprecht, *Europhys. Lett.* **54**, 449 (2001).
- 372 [4] A. Huke, *Die Deuteronen-fusionsreaktionen in Metallen*, PhD Thesis, Technische Universität, Berlin,
373 (2002).
- 374 [5] H. Hora and G.H. Miley, "Heavy nuclide synthesis by neutrons in astrophysics and by screened
375 protons in host metals", *CZEC J PHYS*, 50(3), pp. 433-439, 2000.
- 376
- 377 [6] Szpak, Masier-Boss: Thermal and nuclear aspects of the Pd/D₂O system, Feb 2002. Reported by
378 Mullins 2004.
- 379 [7] F. Raiola et al., *Eur. Phys. J. A* **13**, 377 (2002);
- [8] F. Raiola et al., *Phys. Lett.* **B547**, 193 (2002). 380
- 381 [9] C. Bonomo et al., *Nucl. Phys.* **A719**, 37c (2003).
- 382 [10] F. Raiola et al., *Eur. Phys. J. A* **19**, 283 (2004).

- 383 [11] A. Huke, K. Czerski, and P. Heide, Nucl. Phys. **A719**, 279c (2003).
- 384 [12] P. Kalman and T. Keszthelyi, Phys. Rev. C **69**,031606(R) (2004).
- 385 [13] Broad 1989b, Voss 1999, Platt 1998, Goodstein 1994, Van Noorden 2007, Beaudette 2002, Feder
386 2005, Adam 2005, Kruglinksi 2006, Adam 2005, Alfred 2009
- [14] B. Simon, *Undead Science: Science Studies and the Afterlife of Cold Fusion*, Rutgers, NJ: Rutgers
University Press, 2002. 388
- [15] C. Seife, *Sun in a Bottle: The Strange History of Fusion and the Science of Wishful Thinking*
New York University Press, Oct, 2008, pp. 154–155. 390
- 391 [16] Hubler, G. Anomalous Effects in Hydrogen-Charged Palladium – A Review. *J. of Surface &*
392 *Coatings Technology* 2007 (10.1016/j.surfcoat.2006.03.062)
- 393 [17] K. Czerski *et al.*, Eurouphys. Lett. **54**, 449 (2001); Nucl.Instrum.Methods Phys. B **193**, 183 (2002).
- 394 [18] A. Huke *et al.*, Phys. Rev. C **78**, 015803 (2008).
- 395 [19] A. Huke, K. Czerski, S. M. Chun, A. Biller, and P. Heide, Eur. Phys. J. **A35**, 243 (2008).
- 396 [20] P. Kalman and T. Keszthelyi, Phys. Rev. C **79**, 031602(R) (2009).
- 397 [21] K. Hagino and A. B. Balantekin, Phys. Rev. C **66**, 055801 (2002).
- 398 [22] S. Kimura *et al.*, Phys. Rev. C **67**, 022801 (2003).
- 399 [23]D. L. Walter and J. Wiley, *Modern Nuclear Chemistry*, p. 232, ISBN 0471115320, (2005).
- 400 [24]S. K. Kenneth and J. Wiley & Sons, *Introductory Nuclear Physics*. ISBN 0-471-80553-X, (1988).
- 401 [25] G. Fiorentini *et al.*, Phys. Rev. C **67**, 014603 (2003).
- 402 [26] J. H. Hamilton, *Internal Conversion Processes* (Academic, New York, 1966).
- 403 [27] C. Angulo *et al.*, Nucl. Phys. **A656**, 3 (1999).
- 404 [28] J. M. Ziman, *Principles of the Theory of Solids* (Cambridge University Press, Cambridge, 1964), pp.
405 148-150 .
- 406 [29] K. Alder *et al.*, Rev. Mod. Phys. **28**, 432 (1956).

407

408